2

Automotive Testing in the German-Dutch Wind Tunnels

Eddy Willemsen, Kurt Pengel, Herman Holthusen, Albert Küpper, et al
German-Dutch Wind Tunnels DNW
The Netherlands

1. Introduction

The Foundation German-Dutch Wind Tunnels (DNW) was jointly established in 1976 by the Dutch National Aerospace Laboratory (NLR) and the German Aerospace Centre (DLR), as a non-profit organisation under Dutch law. The main objective of the organisation is to provide a wide spectrum of wind tunnel tests and simulation techniques to customers from industry, government and research. DNW owns the largest low-speed wind tunnel with open and closed test section options in Europe. Also the major aeronautical wind tunnels of the DLR and NLR are fully integrated and managed by the DNW organisation. The wind tunnels are grouped into two Business Units "Noordoostpolder/ Amsterdam" (NOP/ ASD) and "Göttingen und Köln" (GUK).

DNW provides solutions for the experimental simulation requirements of aerodynamic research and development projects. These projects can originate in the research community (universities, research establishments or research consortia) or in the course of industrial development of new products. Most of the industrial development projects come from the aeronautical industry, but the automotive, civil engineering, shipbuilding and sports industries have also benefited from DNW's capabilities.

For efficient and flexible operations, DNW operates in a decentralised structure under a unified management and supervision. The seat of its Management is in Marknesse, at the location of its largest wind tunnel, the DNW-LLF. DNW's Board, the supervisory body of the Foundation, consists of representatives of the parent institutes NLR and DLR, and is complemented by representatives of the relevant ministries from Germany and the Netherlands.

In order to assure the compatibility of DNW's development strategy with the long-term needs of the research and development market, an Advisory Committee consisting of high-level representatives of participants in the market provides strategic advice and information to DNW.

2. The wind tunnels of DNW

The eleven wind tunnels of DNW include low speed, high speed, transonic and supersonic facilities. They are distinguished with three-lettered names. The following wind tunnels are also used for testing ground and rail vehicles:

KKK Cryogenic wind tunnel at Cologne, Germany. A closed circuit, continuous, low-speed wind tunnel with a closed wall test section

LLF Large low-speed facility at Marknesse, the Netherlands. A closed circuit, atmospheric, continuous low-speed wind tunnel with three closed-wall exchangeable test sections and an open jet

LST Low-speed wind tunnel at Marknesse, the Netherlands. A continuous, atmospheric, low-speed wind tunnel with exchangeable test sections

NWB Low-speed wind tunnel at Braunschweig, Germany. A continuous, atmospheric, low-speed wind tunnel with optionally a closed or a slotted test section with an open jet

2.1 The DNW-LLF

The LLF (Fig. 1) is situated near Marknesse, approximately 100 km north-east of Amsterdam. It is an atmospheric, single return wind tunnel with two exchangeable test section arrangements. It can also be operated in the open-jet mode, whereby the complete test section is removed and acoustic measurements in an anechoic environment can be executed. Each test section configuration exists of three elements: a nozzle which forms the connection between the contraction at the end of the settling chamber and the test section, the actual test section itself and the transition which forms the connection between the test section and the diffuser part of the wind tunnel. These three elements have an overall length of about 44 m.

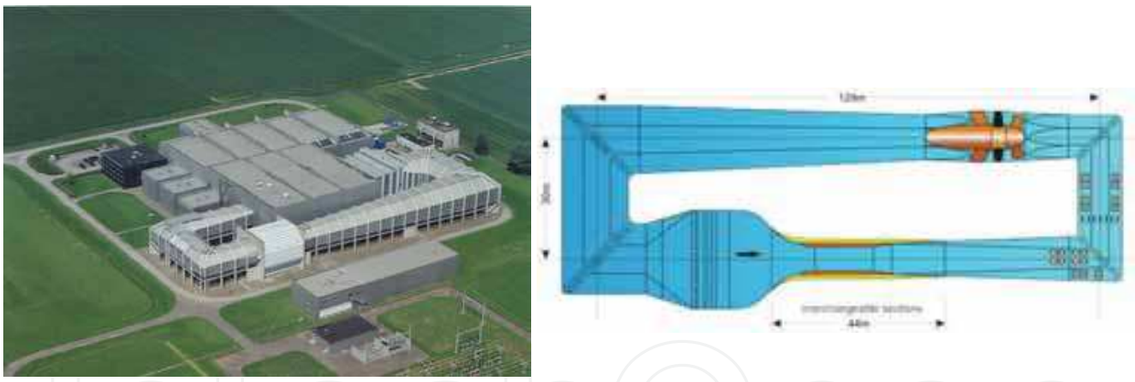

Fig. 1. Aerial view and layout of the LLF circuit

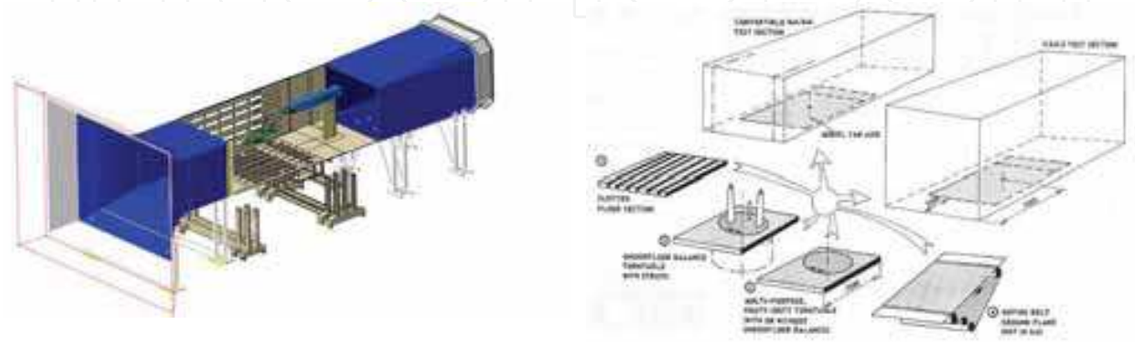

Fig. 2. Test section arrangement (left) and overview of interchangeable floor sections (right)

There are two test sections with different dimensions. The largest one has a cross section of 9.5 m x 9.5 m and the smallest one is convertible between a cross section of either 8 m x 6 m or 6 m x 6 m. These three test sections are further on referred to as the 9.5x9.5, the 8x6 and the 6x6 test section, respectively. Of the convertible test section all four walls have adjustable slots which when opened to their maximum results in 12% porosity. For the open jet arrangement the 8x6 nozzle is used together with the 9.5x9.5 transition. Converting the 8x6 to 6x6 is achieved by mounting inserts in the 8x6 nozzle and moving in the two sidewalls. The 9.5x9.5 and the 8x6 test section have a length of 20 m; the 6x6 is 15 m long. Both test sections rest on air cushions for easy exchangeability.

The air flow in the tunnel is generated by a single stage fan of 12.35 m diameter with eight fixed blades. The fan is driven by a variable speed synchronous motor located in the nacelle with a nominal maximum power of 12.65 MW at 225 rpm.

The maximum wind speed in the 9.5x9.5 test section is 62 m/ s, in the closed 8x6 test section 116 m/ s, in the open 8x6 test section 78 m/ s and in the 6x6 test section 152 m/ s.

The test sections have removable and exchangeable floors (Fig. 2). One of the floor sections has slots (floor #1), one has a 5. 5m diameter turntable for use with the external balance (floor #2) and one has a 5 m diameter multi-purpose turntable (floor #3).

The flow quality of the LLF is very high. The turbulence levels vary with wind speed and are different for the different test sections. At 150 km/ h (42 m/ s) the 8x6 test section has a turbulence level of less than 0.1 percent and the 9.5x9.5 test section of 0.25 percent. This is illustrated in more detail in Figure 3.

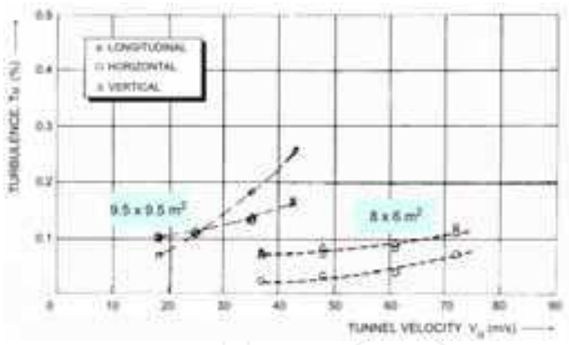

Fig. 3. Turbulence levels

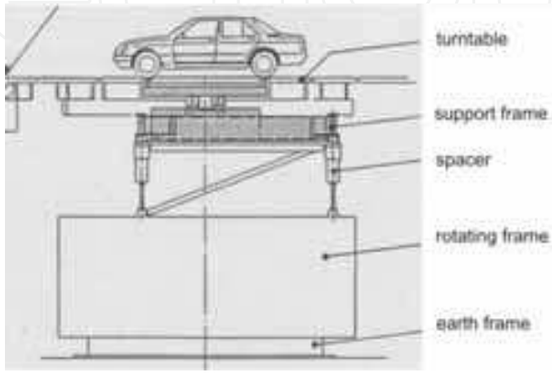

Fig. 4. Setup with the external balance

Fig. 5. Sting support system (left) and truck setup in the 9.5x9.5 test section (right)

LLF has two standard support systems (Fig. 4 and 5):

- A sting support system, to which models are mounted via an internal balance. This is mostly used for aircraft and helicopter testing, but is also necessary for cars in combination with the moving belt (moving ground plane)
- An external under-floor platform type balance with a model support by pads or special adapters. This is mostly the primary choice for cars and trucks

3. Force and moment measurements

Two test sections of 20 m length each are suitable for automotive testing at DNW.
Full-scale cars and vans are often tested in the 8x6 closed test section, where up to 400 km/ h wind speed can be reached. A car platform with adjustable pads is linked to an external underfloor balance for the measurement of six stationary load components, i.e., drag, side force, lift, and the moments in roll, pitch and yaw. The platform can be used in combination with a tunnel floor boundary layer control system which injects pressurized air into the sublayer upstream of the test vehicle to improve the road simulation conditions and can be used in both test sections.
A sting system for internal balance (six-component) supported cars can be used in combination with a moving belt system for perfect road simulation and rolling wheels.
Full-scale trucks and buses use the 9.5x9.5 closed test section, where the maximum wind speed of 200 km/ h is more than enough. A truck platform is available in combination with loose air cushion elements to support the large and heavy vehicles. This setup provides three stationary load components, i.e. drag, side force and yawing moment by means of the external underfloor balance.
The external balance (EXB) is a six-component platform balance, equipped with three horizontal load cells with a resolution of 0.15 N and three vertical load cells with a resolution of 0.30 N. This balance is installed underneath the test section. The test vehicle rests with its wheels on four small pads which are flush with the floor of the turntable and can be adjusted over a wide range to match track and wheelbase. The wheel pads are incorporated in a rigid supporting frame (car platform), which is connected to the metric part of the balance. When use is made of the 8x6 test section, the vertical distance between supporting frame and balance is bridged by a spacer. The balance assembly can rotate over ± 180° in increments of ± 0.1°.

Fig. 6. Model on sting above moving belt

Fig. 7. Truck in 9.5x9.5 test section

4. Road simulation

During wind tunnel tests the relative motion between vehicle and road and the rotation of the wheels is often disregarded. The road is then represented by the rigid floor of the test section and the vehicle rests with stationary wheels on the pads of the balance platform.
The flow pattern around such a configuration is principally different from that on the road due to the grown boundary layer along the wind tunnel floor. The boundary layer thickness near the model may reach a thickness of half the ground clearance of a standard passenger car. This will affect the aerodynamic phenomena around the car.
The effects from various ground simulation techniques at automotive testing in a wind tunnel have been discussed in years around 1990 in various papers of the Society of Automotive Engineers (SAE). Mercker and Knape (1989) discussed the ground simulation with a moving belt or with tangential blowing. Mercker and Wiedemann (1990) compared the results obtained at different ground simulation techniques.

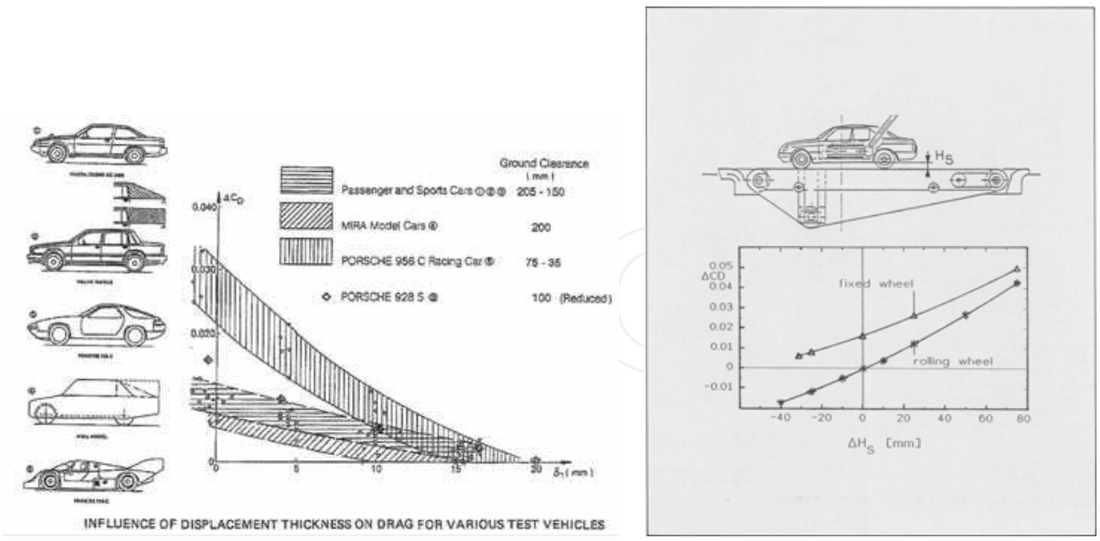

Fig. 8. Effects from ground clearance (left) and rotating wheels (right)

Another deficiency arises from the stationary wheels. Rolling wheels not only affect the flow over and around the wheels but also the overall flow pattern around the car.
As long as the drag of the tested vehicle is relatively high, the error on the drag from the fixed ground floor and the stationary wheels is generally negligible. For vehicles with lower drag this error is not negligible, especially when the low drag is achieved by measures at the underbody of the vehicle. These effects are illustrated in figure 8.
The results from wind tunnel tests can become more realistic when the effect from the boundary layer development along the wind tunnel floor is reduced by boundary layer suction or tangential blowing. Further improvement may be obtained with rotating wheels.

4.1 Tangential blowing

With tangential blowing, air is blown in the direction of the wind through a narrow slot in the wind tunnel test section floor. The blowing device consists of a slot adjustment mechanism and a tubular settling chamber. The principle is that so much air is added to the boundary layer that the momentum deficit in the boundary layer of the wind tunnel floor is reduced to zero. This can be reached exactly at only one downstream distance from the blowing slot.
The system of the LLF is located 4.5 m upstream off the balance centre. The slot spans a length of 6 m and has a variable width between 0 and 5 mm. In order to arrive at a homogeneous spanwise velocity distribution at the exit of the slot, the settling chamber is divided into six individually controlled lateral sections, each provided with a porous smoothing plate. Pressure and temperature are monitored at the centre of the chamber.
The momentum of the thin layer of blown air must be balanced with the momentum of the airflow in the tunnel. From calibration of the blowing device the required ratio V_j / V_0 of the jet velocity V_j at the slot exit to the free stream velocity V_0 is determined as function of the V_0.
Figure 9 shows the setup and calibration results of the tangential blowing system. With tangential blowing good results can be obtained, even for small ground clearances. However, some deformation in the velocity profile remains and the effects from rotating wheels are still ignored.

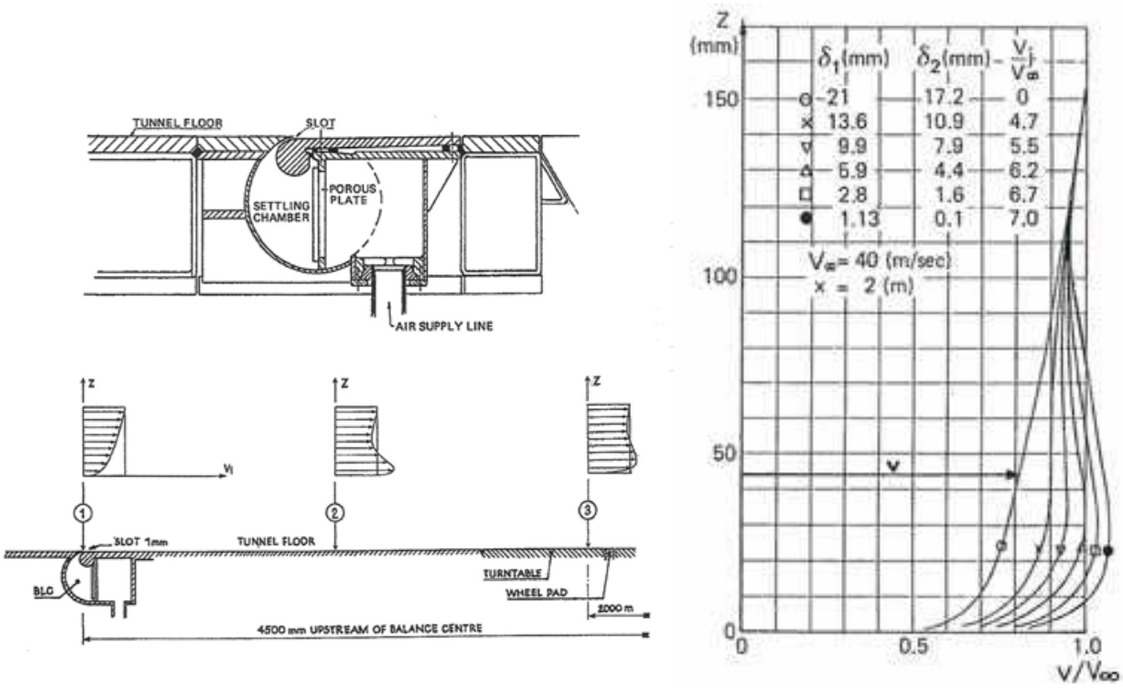

Fig. 9. Tangential blowing system with setup (left) and calibration results (right)

4.2 Moving belt ground plane

The most appropriate way to simulate the full-scale conditions is with a moving belt ground plane. The momentum loss in the boundary layer is almost completely absent over the complete length of the rolling floor and the rotation of the wheels can be enabled as well. However, the disadvantage is that the suspension of the vehicle in the test section is no longer simple.

The moving belt at the LLF has a maximum width of 6.3 m and a flow exposed length between the two main rollers of 7.6 m. Two variable-speed drives of 85 kW each give the belt a maximum speed of 40 m/ s. The belt is tensioned and tracked by means of a third roller. Its flatness is monitored during testing by a video camera and with the aid of a laser beam on the wind tunnel side wall. Even under most severe conditions when the vehicle exerts lift, the belt must remain very flat. To reduce friction, pressurized air is fed between belt and support plate. The upstream ground floor boundary layer is scooped off by raising the whole assembly 200 mm above the tunnel floor. The extracted air re-injects automatically at the rear of the belt assembly and through the test section breathers.

The influence of the scoop and belt motion on the boundary layer properties has been calibrated by measuring the velocity profiles at the front and the rear of the belt. Beside the removal of the boundary layer it is essential that the static pressure in longitudinal direction remains constant over the length of a full size passenger car to avoid buoyancy effects in the drag data. This is effectively controlled by adjusting the rearward flaps of the belt. Figure 10 shows the setup and some flow characteristics of the moving belt ground plane at the LLF.

4.3 Rotating wheels

The effects of rotating wheels on the measured aerodynamic forces can be investigated in combination with a moving belt ground plane that drives the wheels by friction. The car is

mounted to the available sting and forces are measured with an internal balance between sting and car.
Shock absorbers and springs of each wheel are replaced by a dual-action pneumatic cylinder to counterbalance the wheel's weight but still be able to create an effective downward force.
Rolling resistance of the wheels is determined from the internal balance measurement without wind.
In general, the drag is reduced by wheel rotation, but the magnitude of the drag reduction depends strongly on the type of car and on the ground clearance of the vehicle. The closer to the ground, the more pronounced the effect of the rolling wheels will be; see figure 8.

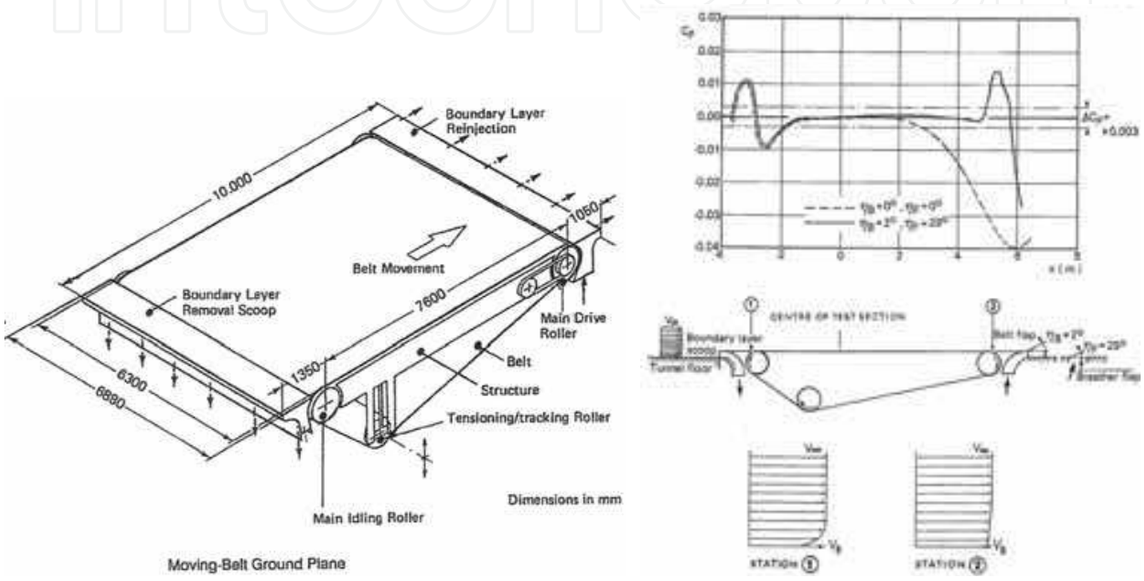

Fig. 10. Setup (left) and velocity profiles (right) of the moving belt ground plane

5. Acoustic measurements

The classical type of acoustic measurements with trucks in wind tunnels is based on the measurement of the noise inside the cabin, as induced by the airflow around the truck and measured with a small number of microphones or with a so-called acoustic head. These cabin noise measurements can be used for the assessment of the acoustic comfort for the truck driver.
The transfer mechanism of the noise from outside the cabin towards cabin interior is often very difficult or impossible to determine. Typical exterior structures are mirrors, the sunscreen above the front window, wind shields, antennas and various spoilers.
Instead of measuring interior cabin noise levels at various exterior configurations, it is more straightforward to measure the exterior sound production. This can be realized with an acoustic mirror or with an array of a large number of microphones.
In an acoustic mirror system a single microphone is mounted in the focal point of a parabolic or elliptic acoustic mirror. Single-microphone measurements give overall noise levels and do not distinct between different noise sources. In a phased microphone system the location and strength of different noise sources can be measured by a phased array technique, whereby on software level the time series of the microphones are analyzed. Similar techniques are applied in radar technology and ultrasonic imaging. A description of

array signal processing is given by Johnson and Dudgeon (1993). A description of applications in a wind tunnel environment is given by Underbrink and Dougherty (1996), Piet and Elias (1997), Sijtsma (1997), Dougherty (1997) and Sijtsma and Holthusen (1999). Figure 11 illustrates the principles of the acoustic mirror and the phased microphone array.

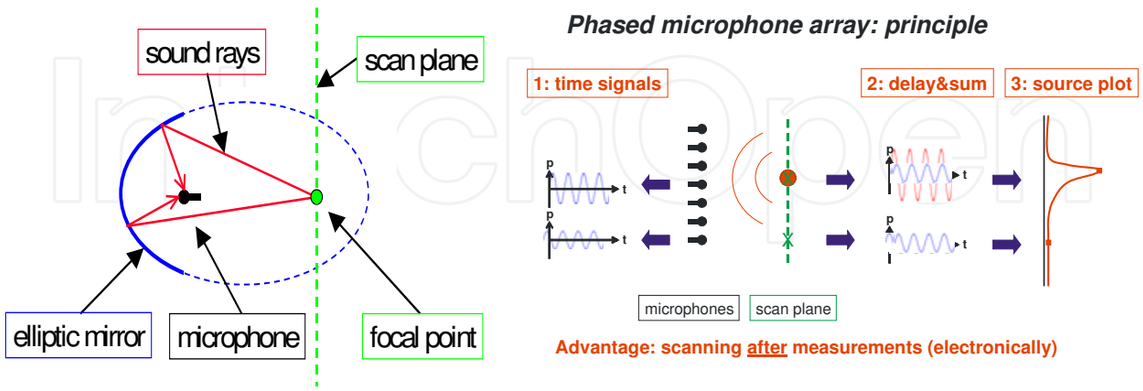

Fig. 11. Acoustic source localization measurement techniques, mirror (left) and acoustic array (right)

Microphone arrays or acoustic mirrors have become popular in wind tunnel measurements as a tool to locate sound sources. Microphone arrays have the advantage over acoustic mirrors of a higher measurement speed. Mirrors have to scan the whole test object point by point, while microphone arrays only need a short time to record the signals from which the aero-acoustic characteristics in a measuring plane can be determined. The process of scanning through possible source locations is performed afterwards by appropriate software running on powerful computer hardware.

An additional advantage of a microphone array is the application inside the flow or in the wall of a closed test section. These in-flow measurements with microphone arrays are possible, when the self-noise of the array microphones, caused by the turbulent boundary layer above the array, is sufficiently suppressed. With a mirror, in-flow measurements are practically speaking impossible.

Fig. 12. Test setup examples: full-scale wing in the LLF (left) and scaled truck model in the LST (right)

In a typical test an array of 1 m diameter, containing about 140 sparsely distributed microphones, may be mounted in or on the wall of the test section.
The microphone array technique can be successfully applied in full-scale tests as well as model tests; see figure 12 for some examples.
The array processing delivers as its main result so-called noise maps. Figure 13 presents some results for a scaled truck and for a full-scale truck. The two dimensional contour maps show the distribution of noise sources in a scanned area near the truck. The noise levels are represented by different colors. The noise maps deliver the location, frequency characteristics and relative strength of the noise source. Additionally the array processing delivers power spectra and overall power levels by integration over the scan area. Several of such scan areas can be defined and processed. One scan area could cover the whole model and other areas could only cover small details, like an outside car mirror, to allow detailed comparisons between different model configurations.

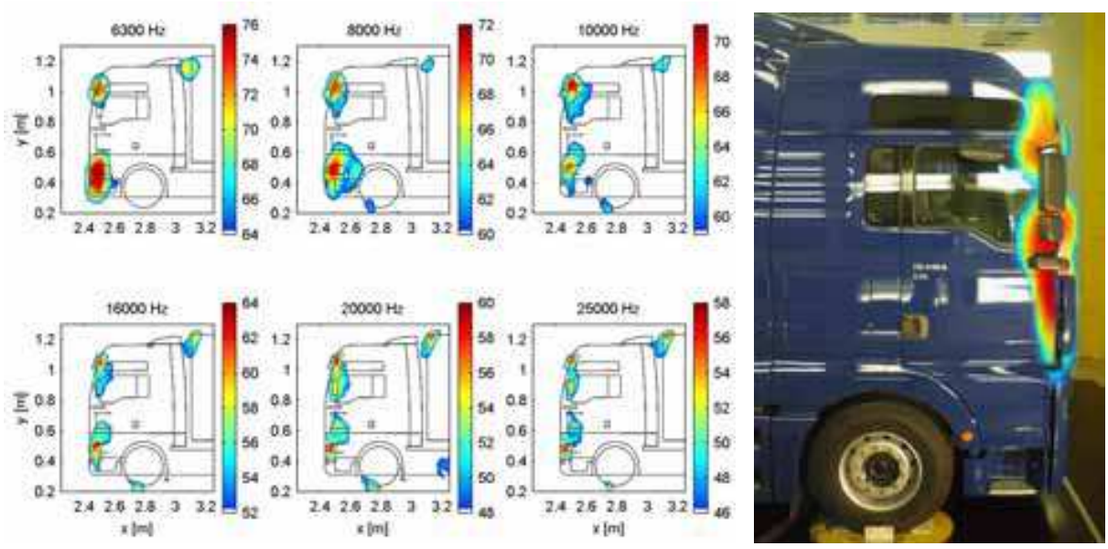

Fig. 13. Microphone array tests results for a scaled truck model (left) and full-scale truck with projected noise map (right)

6. Flow field measurements with a traversing rake of five-hole probes

Quantitative flow field measurements can be executed by means of a traversing rake of multiple five-hole probes. Each five-hole probe can measure the local 3-D wind velocity vector. At each position of the rake the wind speed vector is measured at all probe positions. At DNW there are 18 probes at 15 mm stitch; so each time the data are read out information on a line of 255 mm length are gathered. The rake is normally mounted vertically and connected to a traversing mechanism which is moving at such a low speed that the local flow field is not affected. By repeating the readings during the scan after say every 7.5 mm displacement of the rake and repeating the scan at a vertical displacement of the rake of also 7.5 mm, a block of measuring points is filled with a horizontal and a vertical stitch of 7.5 mm. This is enough to observe flow phenomena on a rather small scale. Software tools may provide additional information, like the strength of the vorticity in the flow. A single scan of about 1 meter at a low traversing speed requires a measuring time of about 10 minutes.

The test technique is providing very nice results in as well a quantitative as a qualitative way. Only close to the surface of the test object the flow may become disturbed by the presence of the rake body close to the object.
An example of the setup in the LST wind tunnel is shown in figure 14, together with some test results behind the wing tip of an aircraft model.

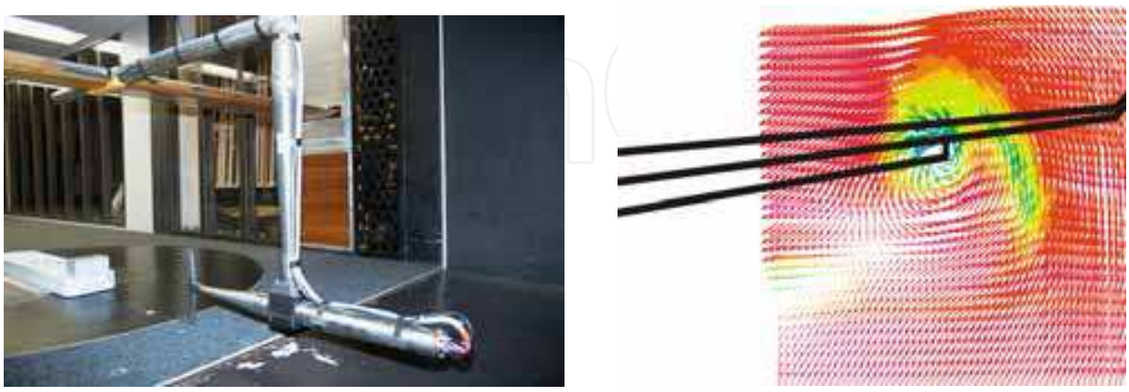

Fig. 14. Test setup in the LST (left) and test results behind the wing tip of an aircraft model (right)

7. Flow field measurements with PIV

The flow field in the vicinity of a test object can be measured by means of Particle Image Velocimetry (PIV); see figure 15.

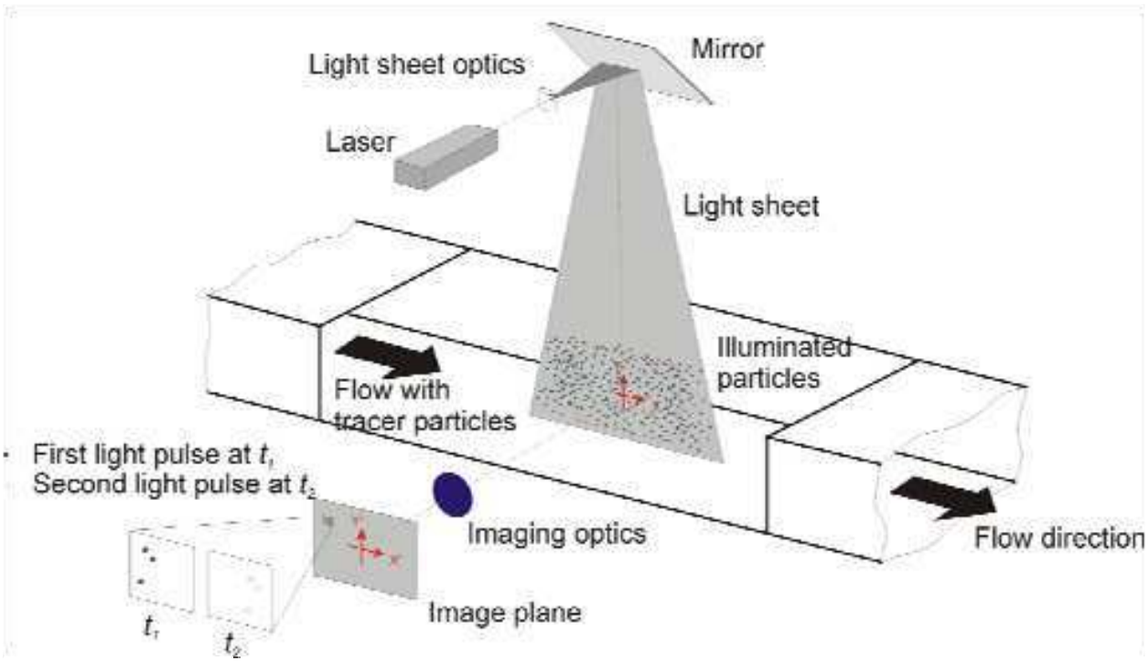

Fig. 15. Experimental setup for PIV

During PIV measurements the flow is seeded with small particles with a diameter in the order of 10 to 100 micrometers (a kind of a light smoke). With a laser two flashing light

planes are created shortly after each other, whereby the light is reflected by the particles. The images are analyzed with a software algorithm, identifying the location of the separate particles during the two images. Once this displacement is established, the corresponding flow speeds in the laser light plane can be calculated. From these wind vector data other characteristic parameters can be calculated, like the vorticity.

The technique and application for a wind tunnel environment became to growth in the last decade of the 20th century. Various authors gave a general description of the principles and possible application at aerodynamic research in wind tunnels, like Willert and Gharib (1991), Adrian (1991), Hinsch (1993), Willert et al. (1996), Willert (1997), Kähler et al. (1998), Raffel et al. (1998), Ronneberger et al. (1998) and Kompenhans et al. (1999).

Figure 16 shows a setup as applied for a wind turbine. A stereoscopic set-up of the cameras enables the determination of the three dimensional flow field characteristics. One camera was directed from above to the horizontal light sheet, the second camera was looking from underneath. This configuration was fixed and could be moved as a whole from one location to another. This fixed set-up of cameras and light sheet allows a system calibration in advance outside the wind tunnel and avoids time consuming re-calibration.

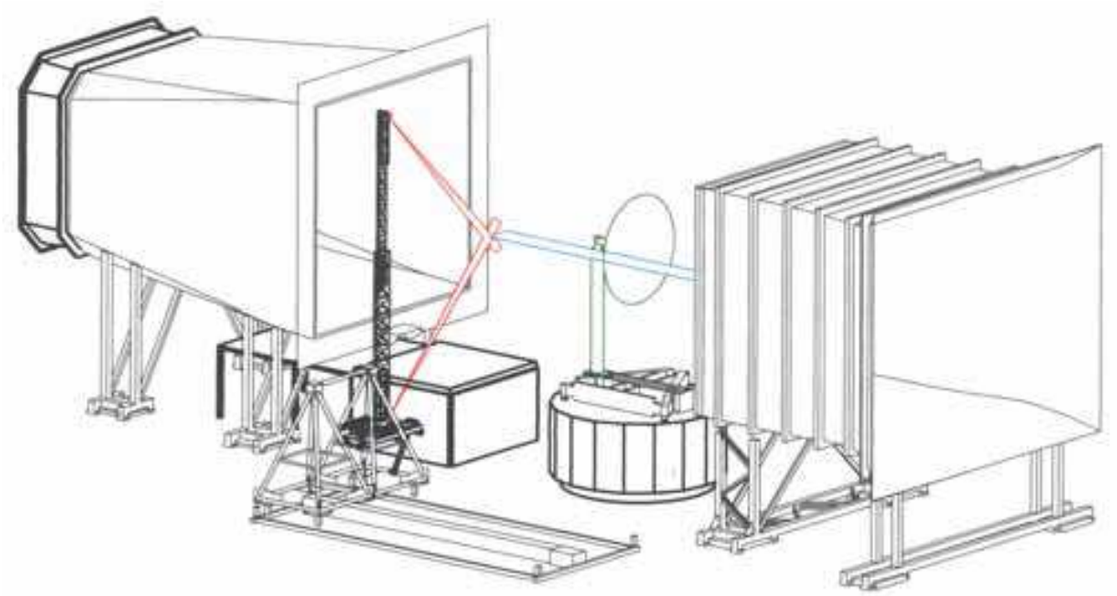

Fig. 16. PIV set-up on a wind turbine

PIV measurements result in vector maps of the velocities in the area where the cameras are focused to. Figure 17 shows some test results at two different setups: underneath a military aircraft and behind the tip of a wind turbine rotor.

The application of PIV in large wind tunnels gives some specific challenges:

- large observation areas requested,
- large observation distances exist between camera and light sheet,
- much time needed for the setup of the PIV system,
- strict safety measures required for laser and seeding,
- high operational costs of the wind tunnel.

In spite of these stringent requirements, the PIV technique is very attractive in modern aerodynamic research. It helps in understanding unsteady flow phenomena such as shear

and boundary layers, wake vortices and separated flows. PIV enables spatially resolved measurements of the instantaneous velocity field within a very short time and allows the detection of large and small scale spatial structures in the flow. The PIV method can further provide the experimental data necessary to the validation of an increasing number of high quality numerical flow simulations.

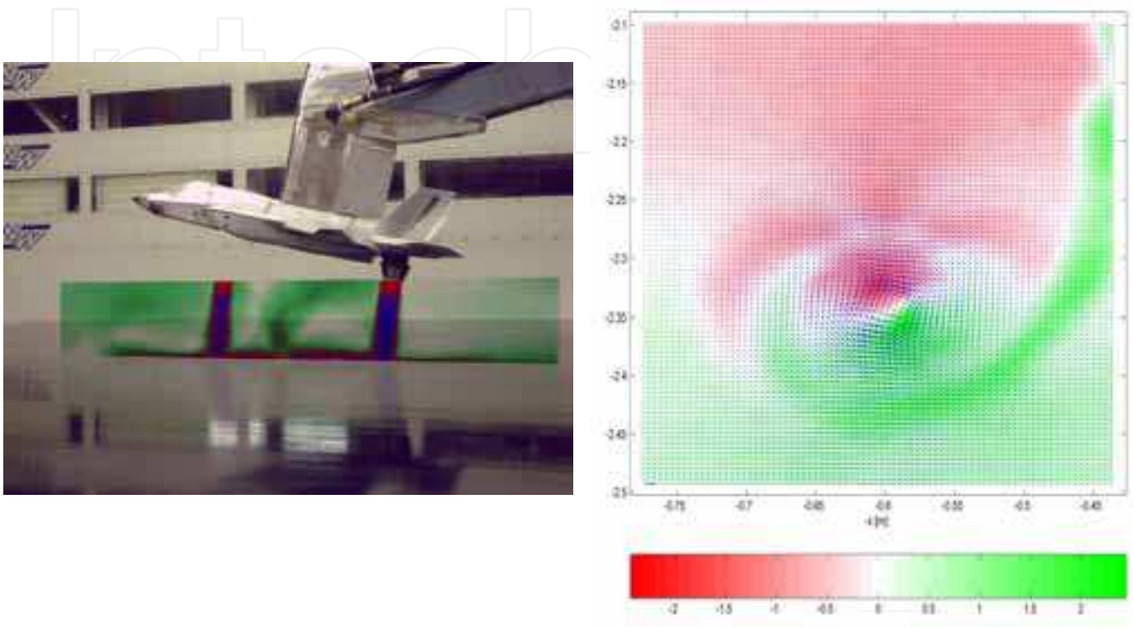

Fig. 17. PIV measurements: exhaust flow of a fighter engine (left) and tip vortex behind a wind turbine rotor (right)

8. Deformation measurements

Within wind tunnel investigations model deformation measurements are possible with techniques like Projection Moiré Interferometry (PMI), Projected Grid Method (PGM) and Stereo Pattern Recognition (SPR) system.
SPR is an optical, non-intrusive method and requires a stereo setup of cameras; it is based on a three-dimensional reconstruction of visible marker locations by using stereo images. Stereo imaging and 3D-reconstruction can be used to determine object locations and their motion with time. There are two possible approaches. If the positions of two (or more) cameras and their optical characteristics are known exactly, a three-dimensional reconstruction is very straightforward. From two images of a certain marker on the object in three-dimensional space by two cameras, the location of this marker can be determined by regarding the images as a result of certain translations and rotations and a final projection on the camera image plane. After calculating transformation matrices for both cameras, derived from the exact set up of the camera positions, the transformation equations for each marker image can be constructed, resulting in an equation system that can be solved by a "least square"-method. A disadvantage of this direct method is that normally the camera positions are not known very exactly. Especially the direction of the optical axis of the cameras and the rotation about this axis can only be measured approximately. In this case a different approach can be used; see figure 18.

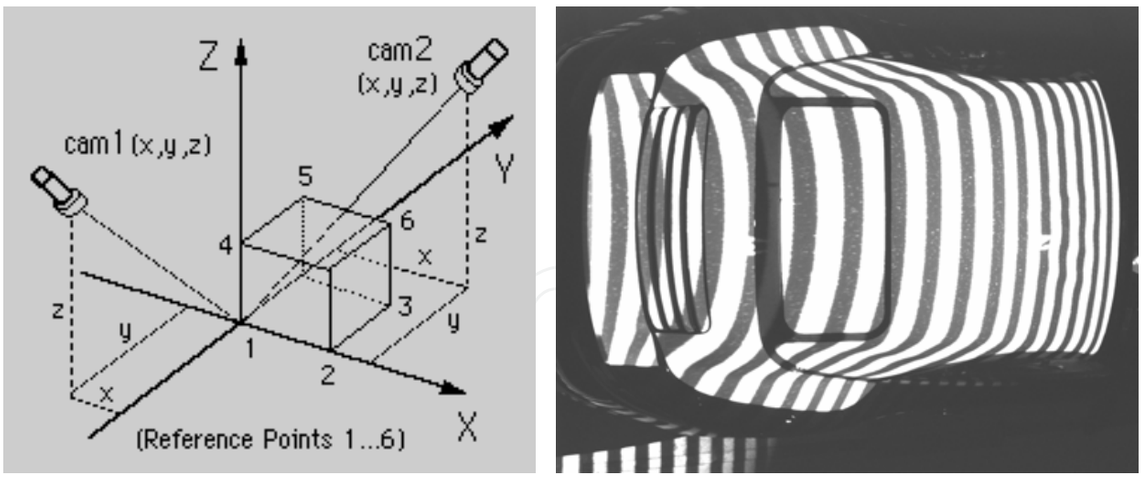

Fig. 18. Setup for SPR with six markers (left) and car roof deformation measurement results from PGM (right)

The transformation matrices can be calculated if the locations of at least 6 markers are known exactly in 3-dimensional space and their images can be detected in both camera views.
Tests have shown that an accuracy of 0.01% of the complete object space can easily be obtained. Measurement accuracy is better than 0.4 millimetres.

9. Flow visualisation techniques

A commonly used flow visualization instrument is a hand-held smoke rod. Oil is ejected through a heated, small tube, whereby the oil is evaporated. Using non-coloured oil results in white smoke, that follows the major flow streamlines and fills wakes and separation zones with smoke.

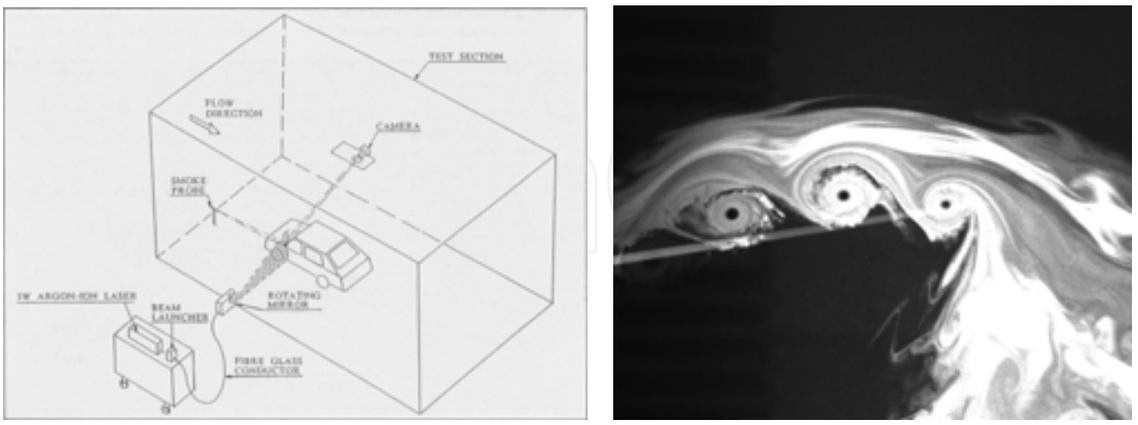

Fig. 19. Laser stroboscope technique; setup with rotating mirror (left) and frozen flow field showing vortices (right)

In combination with a laser light sheet the flow structure is made visible within that plane. A laser light sheet can be created when a laser beam is diverged through a circular cylindrical lens. It is also possible to reflect the laser beam on a rotating mirror. The continuously rotating

laser beam gives the same effect as a laser light sheet, provided that the rotational speed is high enough. By varying the rpm value of the mirror, stroboscopic effects are achieved and periodic flow phenomena can be analyzed. Figure 19 shows a sketch of the setup of the laser light sheet by means of a rotating mirror and an example of vortices visualized with this technique.
Other techniques to visualize the flow are using tufts or oil on the surface of the test object. Tufts are small filaments of cotton or plastic, which are mounted on the surface with magic tape or alike. Tufts follow the local streamlines along the body or behave like small waving flags in separated flow regions. Depending on the material, the tufts may reflect ultraviolet light. Tufts are easy to mount and provide useful basic information. They can be used in a continuous way when the flow direction is changed.
Another technique to visualize the flow is by using a kind of oil on the surface. Depending on the applied oil, transition zones from laminar to turbulent flow may become visible or the separation zones of the flow. Certain oils also reflect ultraviolet light, enhancing the pictures.
Disadvantages of using oil are among others the contamination of the wind tunnel and the test time needed to establish a well-developed oil pattern.

10. Wind tunnel blockage corrections

Testing vehicles in a wind tunnel introduces disturbing effects from the finite dimensions of the airflow. In case of a ¾ open test section the flow from the exit nozzle may have some divergence, leading to a streamline divergence near the vehicle which is somewhat larger than in the unconfined real condition. This results in too low wind loads. In case of a closed test section the streamline divergence near the vehicle is reduced because of confinement by the wind tunnel walls. This results in an increase of the kinetic pressure at the tested object and thus an increase of the measured wind loads.
Corrections are needed, especially for closed test sections and relative large vehicles compared to the wind tunnel cross section dimensions.
In case of a closed test section it is possible to correct by measuring wall pressures in the vicinity of the vehicle. This is however rather elaborate and not common practice. More usual is to correct the reference kinetic pressure analytically, e.g. by a formula that incorporates the measured drag. This latter correction method is basically a base-pressure correction method that started with the work of Maskell (1963), Gould (1969) and Awbi (1978). An empirical blockage correction for trucks in the LLF wind tunnel is described by Willemsen and Mercker (1983). A description of a blockage correction method for automotive testing in a wind tunnel with closed test section is described by among others Mercker (1986).

11. References

Adrian, R. J. (1991), Particle-imaging techniques for experimental fluid mechanics, *Annual Reviews Fluid Mechanics*, Vol. 23, pp. 261-304.

Awbi, H.B. (1978), Wind tunnel wall constraint on two-dimensional rectangular section prisms.

Dougherty, R.P. (1997), Source location with sparse acoustic arrays; interference cancellation, presented at the *First CEAS-ASC Workshop: Wind Tunnel Testing in Aeroacoustics*, Marknesse.

Gould, R.W.F. (1969), With blockage corrections in a closed wind tunnel for one or two wall-mounted models subject to separated flow, *Aeronautical Research Council Reports and Memoranda*, no. 3649.

Hinsch, K.D. (1993), Particle image velocimetry, *Speckle Metrology*, Ed. R.S. Sirohi, pp. 235-323, Marcel Dekker, New York.

Johnson, D.H., Dudgeon, D.E. (1993), Array Signal Processing, Prentice Hall.

Kähler, C.J, Adrian, R.J, Willert, C.E. (1998), Turbulent boundary layer investigations with conventional- and stereoscopic particle image velocimetry, *Proceedings 9th International Symposium on Application of Laser Techniques to Fluid Mechanics*, Lisbon, paper 11.1.

Kompenhans, J., Raffel, M., Dieterle, L., Dewhirst, T., Vollmers, H., Ehrenfried, K., Willert, C., Pengel, K., Kähler, C., Schröder, A. and Ronneberger, O. (1999), Particle image velocimetry in aerodynamics: technology and applications in wind tunnels, *Journal of Visualization*, Vol. 2.

Maskell, E.C. (1963), A theory of the blockage effects on bluff bodies and stalled wings in a closed wind tunnel, *Aeronautical Research Council Reports and Memoranda*, no. 3400.

Mercker, E., Knape, H.W. (1989), Ground simulation with moving belt and tangential blowing for full-scale automotive testing in a wind tunnel, *SAE Paper* 890367, Detroit.

Mercker, E., Wiedemann, J. (1990), Comparison of different ground simulation techniques for use in automotive wind tunnels, *SAE Paper* 900321, Detroit.

Mercker, E. (1986): A blockage correction for automotive testing in a wind tunnel with closed test section, *Journal of Wind Engineering and Industrial Aerodynamics*, 22.

Piet, J.F., Elias, G. (1997), Airframe noise source localization using a microphone array, *AIAA Paper* 97-1643.

Raffel, M., Willert, C., Kompenhans, J. (1998), Particle image velocimetry - a practical guide, Springer Verlag, Berlin.

Ronneberger, O., Raffel, M., Kompenhans, J. (1998), Advanced evaluation algorithms for standard and dual plane particle image velocimetry, *Proceedings 9th International Symposium on Application of Laser Techniques to Fluid Mechanics*, paper 10.1, Lisbon.

Sijtsma, P., Holthusen, H. (1999), Source location by phased array measurements in closed wind tunnel test sections, NLR-TP-99108.

Sijtsma, P. (1997), Optimum arrangements in a planar microphone array, presented at the *First CEAS- ASC Workshop: Wind Tunnel Testing in Aeroacoustics*, Marknesse.

Underbrink, J.R.; Dougherty, R.P. (1996), Array design of non-intrusive measurement of noise sources, Noise-Conference 96, Seattle, Washington.

Willemsen, E., Mercker, E. (1983), Empirical blockage corrections for full-scale automotive testing on straight trucks in a wind tunnel, NLR TR 83065 L.

Willert, C., Raffel, M., Kompenhans, J., Stasicki, B., Kähler, C. (1996), Recent applications of particle image velocimetry in aerodynamic research, *Flow Measurement and Instrumentation*, Vol. 7, pp. 247 -256.

Willert, C. (1997), Stereoscopic digital particle image velocimetry for application in wind tunnel flows, *Measurement, Science and Technique*, Vol. 8, No. 12., pp. 1465 – 1479.

Willert, C.E., Gharib, M. (1991), Digital particle image velocimetry, *Experiments in Fluids*, Vol. 10, pp. 181-183.

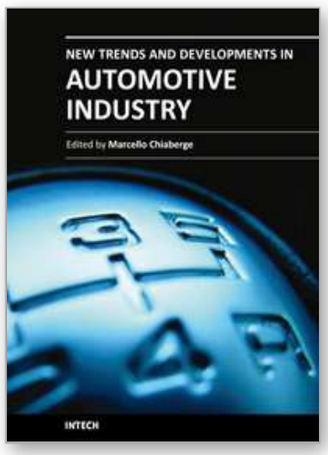

New Trends and Developments in Automotive Industry
Edited by Prof. Marcello Chiaberge

ISBN 978-953-307-999-8
Hard cover, 394 pages
Publisher InTech
Published online 08, January, 2011
Published in print edition January, 2011

This book is divided in five main parts (production technology, system production, machinery, design and materials) and tries to show emerging solutions in automotive industry fields related to OEMs and no-OEMs sectors in order to show the vitality of this leading industry for worldwide economies and related important impacts on other industrial sectors and their environmental sub-products.

How to reference
In order to correctly reference this scholarly work, feel free to copy and paste the following:

Eddy Willemsen, Kurt Pengel, Herman Holthusen and Albert Küpper (2011). Automotive Testing in the German-Dutch Wind Tunnels, New Trends and Developments in Automotive Industry, Prof. Marcello Chiaberge (Ed.), ISBN: 978-953-307-999-8, InTech, Available from: http://www.intechopen.com/books/new-trends-and-developments-in-automotive-industry/automotive-testing-in-the-german-dutch-wind-tunnels

INTECH
open science | open minds

InTech Europe
University Campus STeP Ri
Slavka Krautzeka 83/A
51000 Rijeka, Croatia
Phone: +385 (51) 770 447
Fax: +385 (51) 686 166
www.intechopen.com

InTech China
Unit 405, Office Block, Hotel Equatorial Shanghai
No.65, Yan An Road (West), Shanghai, 200040, China
中国上海市延安西路65号上海国际贵都大饭店办公楼405单元
Phone: +86-21-62489820
Fax: +86-21-62489821

IntechOpen